Ain Shams Engineering Journal (2015) 6, 851–863

Ain Shams University

Ain Shams Engineering Journal

www.elsevier.com/locate/asej
www.sciencedirect.com

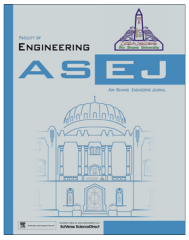

ELECTRICAL ENGINEERING

NSGA-II based optimal control scheme of wind thermal power system for improvement of frequency regulation characteristics

S. Chaine, M. Tripathy *, S. Satpathy

Department of Electrical Engineering, Veer Surendra Sai University of Technology, Burla, Odisha 768018, India

Received 17 September 2014; revised 18 December 2014; accepted 13 January 2015
Available online 7 March 2015

KEYWORDS

Doubly fed induction generator;
Frequency regulation;
AGC;
Wind energy conversion systems;
Non-dominated sorting genetic algorithm-II

Abstract This work presents a methodology to optimize the controller parameters of doubly fed induction generator modeled for frequency regulation in interconnected two-area wind power integrated thermal power system. The gains of integral controller of automatic generation control loop and the proportional and derivative controllers of doubly fed induction generator inertial control loop are optimized in a coordinated manner by employing the multi-objective non-dominated sorting genetic algorithm-II. To reduce the numbers of optimization parameters, a sensitivity analysis is done to determine that the above mentioned three controller parameters are the most sensitive among the rest others. Non-dominated sorting genetic algorithm-II has depicted better efficiency of optimization compared to the linear programming, genetic algorithm, particle swarm optimization, and cuckoo search algorithm. The performance of the designed optimal controller exhibits robust performance even with the variation in penetration levels of wind energy, disturbances, parameter and operating conditions in the system.

1. Introduction

With ever increasing power demand and wide varieties of constraints the capacity expansion of existing power system has created the need of integrating Wind Energy Conversion Systems (WECS) with conventional power grid. Increasing levels of wind generation have resulted in an urgent need for the assessment of their impact on frequency control of power systems. As the penetration of the wind power into the grid increases, their contribution to ancillary services (e.g. voltage and frequency control) becomes more significant and new concerns in the performance of the primary frequency regulation system arise. To analyze the operational issues of the integrated system in a secure manner, research work in the area of Automatic Generation Control (AGC) of power system with considerable penetration of WECS becomes the key area of focus. Among different types of WECS, the more prevalent types based on variable speed wind turbine (VSWT), have

* Corresponding author. Tel.: +91 663 2430055.
E-mail addresses: sabitachaine@yahoo.com (S. Chaine), manish_tripathy@yahoo.co.in (M. Tripathy), satyajits880@gmail.com (S. Satpathy).

Peer review under responsibility of Ain Shams University.

ELSEVIER Production and hosting by Elsevier

http://dx.doi.org/10.1016/j.asej.2015.01.011

power electronic interfaces which along with the pitch angle control enables their rotational speed to remain decoupled from the grid frequency. Unlike conventional thermal power based generators, wind farms respond differently to the variations in network frequency even though their capacity to ramp up/down real power generation maintaining reserve margin is always possible [1]. They have been depicted to participate in system frequency support [2], in the event of any such requirement. VSWTs driving Doubly Fed Induction Generators (DFIG) are designed to regulate their rotational speed in wider ranges by utilizing their stored rotational kinetic energy to facilitate short term active power support in the event of network frequency excursions [3].

With larger penetration of wind farms based on DFIG, the overall natural inertial response capability of the system reduces. This is due to the fact that the power electronics converters decouple the natural dynamics of $\Delta P \sim \Delta f$ that is found in the conventional generators. It prevents them from responding to the changes in system frequency. However, by introducing an additional supplementary control mechanism in DFIG controllers the inertial response capability of the system can be restored [4–7]. In [4], a proposed current controller facilitates inertial response from a DFIG-based system by providing pseudo-hidden inertia to the system. The work in [5], has tried to explore the possibility of providing greater leverage in the rotor speed variation so that considerably more kinetic energy available from the turbine-DFIG units may be utilized. Control strategies which incorporates additional network frequency dependent control signal in their structure, have been suggested in [6,7] to provide short-term frequency regulation. Further, work in [8] proposes to emulate the proportional control implemented in conventional generators to achieve primary frequency regulation. Similarly, work in [9], proposes a method, which not only modifies the inertial control scheme to partially utilize the stored kinetic energy of WECS, but also suggests the WECS response to be communicated to the conventional units so that they can take care of the load imbalance. The impact of different levels of wind penetration resulting in varying degrees of active power support from DFIG based wind farms, on its frequency response characteristics are analyzed in a two thermal area AGC [10].

Looking at the past research, it is therefore necessary to design efficient controllers of WECS, to achieve better frequency regulation of the integrated system without interfering with the performance of AGC controllers adversely. Therefore, the gains and time constants related to any controller could be properly tuned so that they exhibit consistency and robustness under different conditions. The process of tuning may be addressed in the domain of optimization, using any particular algorithm. During recent past, many intelligent technique based optimization techniques like Genetic Algorithm (GA) [11], Particle Swarm Optimization (PSO) [12], Cuckoo Search Algorithm (CSA) [13] and Linear Programming (LP) [14] have been extensively utilized for optimizing varieties of non-linear and non-convex power system problems, including the AGC [11,12]. However, looking at the conflicting natures of different types of objectives in AGC, and differences in the behavior of response of WECS and thermal systems, it may be beneficial to use a multi objective optimization algorithm [15,16]. The Non dominated Sorting Genetic Algorithm-II (NSGA-II) [15], was shown to give better efficiency compared to similar earlier versions and it has provided better solutions. In the view of above discussion, the objectives of the present paper are as follows.

(i) To propose a control scheme that can effectively extract the kinetic energy from DFIG, in order to prevent the initial frequency fall during load perturbation.
(ii) To tune the various controller parameters of AGC and the inertial control blocks of DFIG simultaneously in a coordinated manner, with the help of multi-objective optimization known as NSGA-II. A multi objective optimization may be necessary, since the controllers of DFIG and thermal units operate in different time frames of interest. The controller of DFIG is needed only for a transient period but the integral gains of AGC are required throughout the period of dynamics.
(iii) To compare the optimization efficiency of NSGA-II, with those of several conventional and intelligent techniques based optimization algorithms like, LP, PSO, GA and recently proposed CSA.

For the study, a two area thermal system with the penetration of wind power is considered. The work is organized as follows. In Section 2, a general overview of frequency control aspects of DFIG is discussed. Section 3 introduces the system model with its main components. Section 4 discusses about the objective function that is optimized to maximize the performance of the DFIG in the AGC. A brief overview of the intelligent techniques is elaborated in Section 5. The simulation and results obtained following several tests related to the performance of the DFIG controller are explained and analyzed in Section 6. At the end, conclusions are presented in Section 7.

2. Frequency control aspects of DFIG

The primary frequency control is implemented to compensate the imbalance between the real power load demand and generation in an interconnected power system. It has been a general practice, that the variable speed wind turbines are controlled to utilize the maximum power available from the wind energy. Therefore, any further increase in the generation of power is not possible, so that the DFIG can participate in the secondary control of frequency deviation, unlike the thermal units. However, the stored kinetic energy in the inertia of WECS could be utilized to provide a transient nature of primary frequency control in the interconnected system. Permanent active power controllability in WECS units can only be achieved by regulating either the pitch angle or the speed of the wind turbine. Different types of control methods are briefly reviewed in [17]. Proposed inertial control scheme allows the kinetic energy stored in the rotational masses to provide improved frequency support by the DFIG. The response of the later is also communicated to the conventional generators to help in coordinating their controls.

3. Two area thermal systems with DFIG based wind power generation

The linearized model for the load frequency control of two-area interconnected power system having both thermal and wind power resource is depicted in Fig. 1. As highlighted in the figure the generators for wind power in both the areas

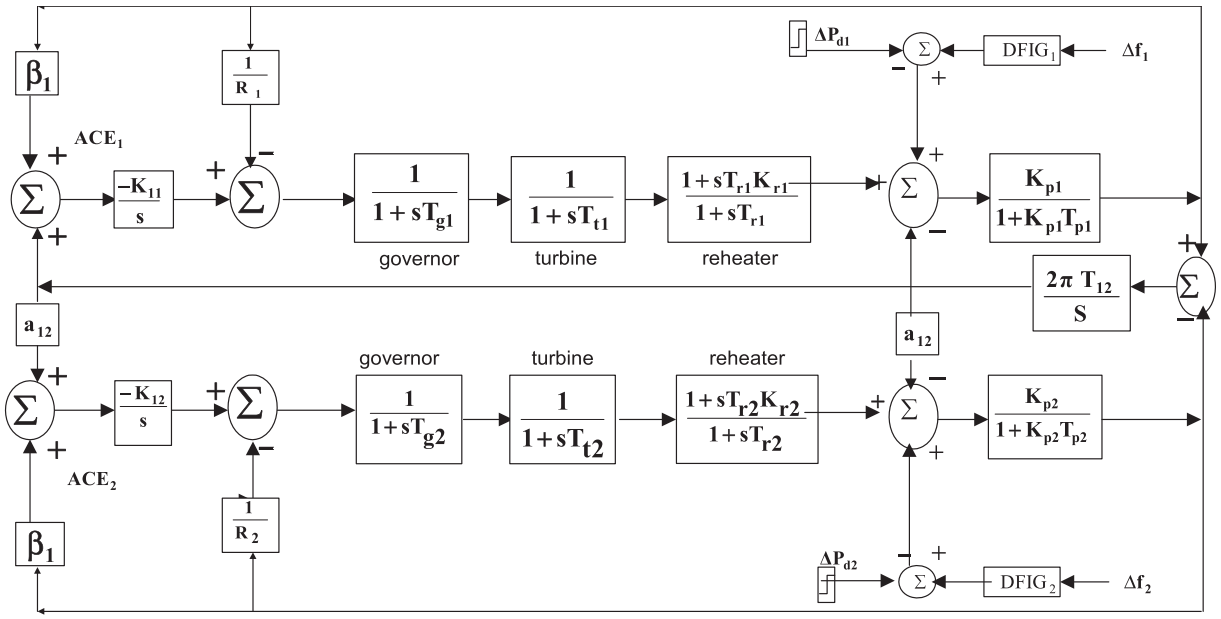

Figure 1 Two area interconnected power system with DFIG.

are DFIGs which can feed real power through both stator and rotor of the induction generator interfacing through two back to back power electronics converters. The converters are interlinked with a capacitor as depicted in Fig. 2. During normal conditions, the converters enable the variable speed wind turbines to capture wind energy over a wide range of wind speeds, generally following the scheme of maximum power point tracking (MPPT). During intermittent wind conditions and after any disturbance in the grid, the controllers for both the converters achieve a fast control of active and reactive power output by following suitable control strategies.

The real power control capacity of DFIG makes it suitable for its use in frequency regulation of the system. Similar to the conventional generators, wind turbines have a significant amount of kinetic energy stored in the rotating mass of their blades. For a given step change in the load ΔP_L, at a wind penetration level (L_p), the inertial contribution from the wind farm can be suitably increased by imposing an increased power step beyond the steady state power setting. The corrected power setting can be fed to the controller of the grid side converter of DFIG to extract more rotational energy from the rotor blades [10,18].

The values of system inertia (H) and regulation droop (R) of the combined wind thermal system change with the variation in L_p [10]. The new altered values of R and H as shown in Table 1, reproduce the equivalent effect of DFIG in the linearized model of the test system.

3.1. Proposed DFIG controller

Three type of control can be adopted to control the system frequency in wind integrated thermal power system.

(1) Inertia control.
(2) Pitch angle control.
(3) Speed control using deloaded power extraction curve.

In this work only inertial control is taken into account, which essentially has two different controller blocks and one

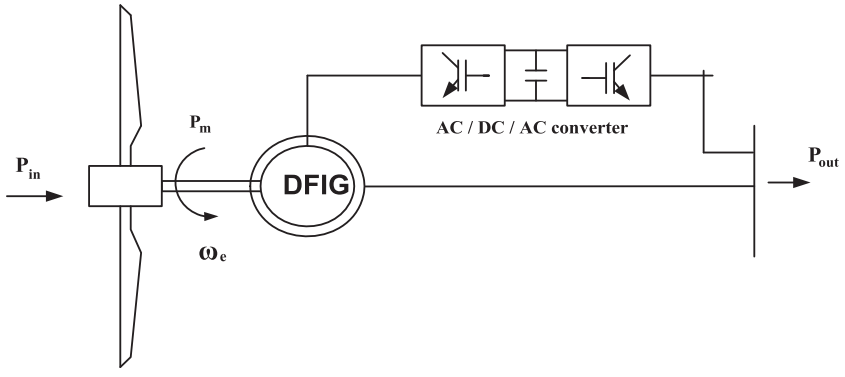

Figure 2 Schematic diagram of DFIG-based wind generation system.

Table 1 Change in values of R and H of the thermal units with different wind penetration by DFIG.

L_p	0%	With frequency support			Without frequency support		
		10%	20%	50%	10%	20%	50%
R	2.4	2.66	3	4.8	2.66	3	4.8
H	5	4.86	4.71	4.015	4.5	4	2.5

wash out filter block. A brief description about each of the blocks is presented as follows.

3.1.1. Proportional derivative (PD) controller

In case of variable speed wind turbines driving the DFIG, the rotational kinetic energy will not naturally contribute to the inertia of the grid as the rotational speed is decoupled from the grid frequency by the grid side converter. Therefore, to emulate the inertia and to facilitate the excess active power injection from the wind turbine for frequency support, an additional auxiliary signal is augmented as depicted in Fig. 3. It can be seen from the figure that, the proposed controller of DFIG meant for providing inertial control adds a signal defined in Eq. (1), to the power reference output that is being tracked by the equivalent controller of the nonconventional machine [7,19,20].

$$p_f^* = -K_{df}\frac{d\Delta f_0{}'}{dt} - K_{pf}\Delta f_0{}' \tag{1}$$

where K_{pf} and K_{df} are the proportionality constants of the frequency deviation and its derivative respectively. In Fig. 3, to control the transient frequency deviations PD controller is used as depicted in Eq. (1). As the grid frequency exceeds certain limits, this additional PD controller is activated, by adding the signal to the torque equation to set the torque demand. As load increase, the system frequency drops, the set point torque is increased and the rotor slows down and kinetic energy is released.

3.1.2. Proportional integral (PI) controller

After the transient period is over, the optimal speed of the nonconventional generator can be retained by using a PI controller. The design constants (K_{wp}, K_{wi}) of the PI controller should be chosen in order to allow fast speed recovery with shorter period of transient speed variation [9]. If the speed is allowed to reduce for longer duration by contributing in the frequency regulation, then the machine may enter the phase of stalling. Therefore, when the system frequency reaches a new steady state that is slightly less than the nominal value, the frequency deviation is regulated by the load damping as well as generator's speed-droop effects.

3.1.3. Washout filter

A washout block, as depicted in Fig. 3, aborts the use of DFIG in its contribution of system frequency regulation for a longer duration. Nonconventional generators cannot afford a permanent system frequency deviation, since they can only act in a transient period by using the stored kinetic energy. The frequency term used is the result of a washout filter (High pass filter), so that permanent frequency deviation has no effect on the control strategy [9].

Moreover, the integral controller (K_i) in AGC loop of the conventional generating units eliminates any steady state error in frequency deviation. As a result, an additional power demand on the convertor controller that is function of frequency deviation is eliminated. After the initial transient period, the normal operation of the DFIG will be restored as DFIG without any frequency support capability.

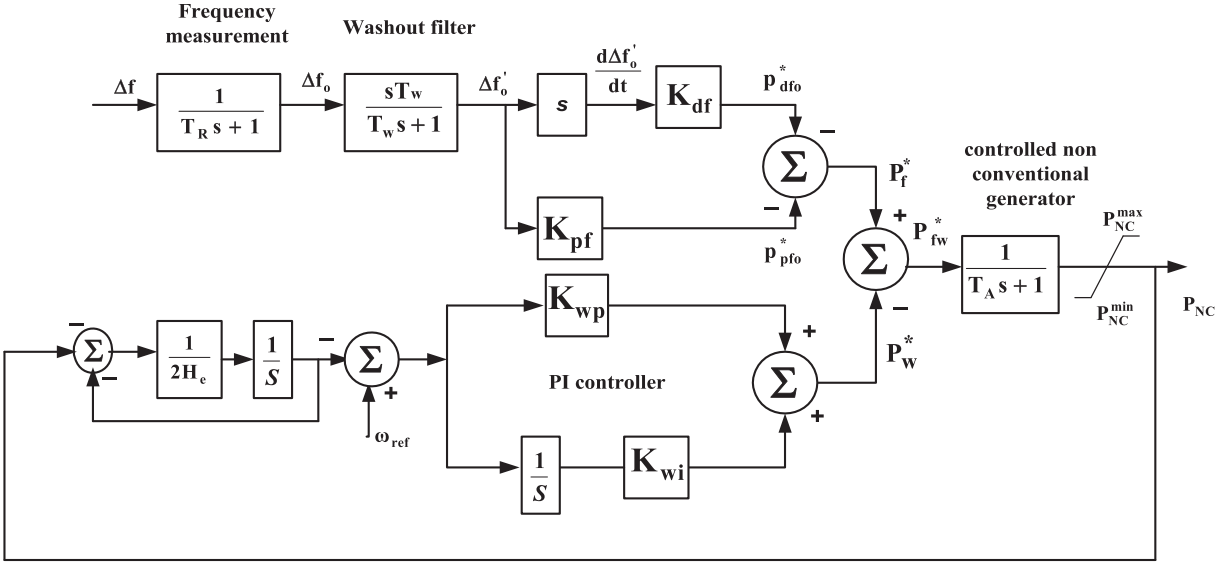

Figure 3 Proposed controller for frequency support in DFIG based WECS.

The values of all the time constants and the power limit of nonconventional generation are given in Appendix A.

4. The methodology of formulation of the objective function

The primary objective of this work is to identify suitable control gains of both the conventional and DFIG controllers whose values affect the nature of frequency deviation and to tune them effectively. Therefore, some of the most sensitive gains of the controllers are to be selected and optimized within a defined optimization framework. For the success of any optimization problem, the suitable design of objective function is an important issue. There are widely accepted performance indices generally used for the purpose of the controller gain optimization in AGC. Four of them are Integral time square error (ITSE), Integral square error (ISE), Integral time absolute error (ITAE) and Integral absolute error (IAE), where the error is that of the frequency deviations. They are explained in Appendix A. To choose a suitable performance index among these four, the parameters of the controllers are optimized using each of them as an objective function separately. The optimization is carried out using the LP algorithm. The gains obtained by optimizing each of the above objective functions are then compared in terms of their damping performance, when a 2% Step Load Perturbation (SLP) in the 1st area is introduced. Analyzing the frequency deviations shown in Fig. 4, it is observed that the set of controller gains obtained by minimizing the ITSE has produced a better dynamic performance in terms of settling time, overshoot and undershoot. Therefore, the time domain performance index ITSE is chosen as one of the several important objectives which would be considered in the formulation of the new objective function.

4.1. Objective function formulated as a single objective

The optimization problem aims to optimize the controller gains of both the DFIG and AGC systems simultaneously so that they coordinate with each other. The objective function is made as a single objective, by combining the performances indices obtained from both time and frequency domain responses of the integrated system. The objective function J, is formulated by using the values of ITSE, total settling times (T_s) of both the area frequency deviations Δf_1, Δf_2, the ΔP_{Tie}, and the minimum damping ratio (MDR) of the eigen values of the system, as defined in Eq. (2).

$$J = \omega_1(\text{ITSE}) + \omega_2(1/X) + \omega_3(T_s) \tag{2}$$

ω_1, ω_2 and ω_3 are the weighing factors suitably chosen.
X = MDR among all the eigenvalues of the system.
T_s = Settling time given below.

$$T_s = T_{sf1} + T_{sf2} + T_{s\Delta Ptie} \tag{3}$$

$T_{S_{\Delta Ptie}}$ = Settling time of tie line power deviation.
T_{sf1} = Settling time of frequency deviation in area 1.
T_{sf2} = Settling time of frequency deviation in area 2.

4.2. Multi objective optimization

Instead of algebraic combination of different types of performance indices as done earlier, a compromising solution may be sought using the technique of multi objective optimization. Looking at the different natures of controllers of DFIG and AGC, this may be more pertinent for this work. The optimization is carried out after obtaining the Pareto optimal solution set of all the probable solutions [21]. Among different approaches some important ones are technique of *scalarization*, *ε-constraints*, *goal programming* and *multi-level programming*, etc. adopted to obtain the multi objective solution using the Pareto optimality. The algorithm NSGA-II has also been used [22,23], in different problems. Each of the three different objectives which are combined to formulate the single objective based function, are considered as multiple objectives simultaneously. A fuzzy-based membership value assignment technique is employed to choose the best compromise solution from the obtained Pareto solution set [23]. Some elementary discussions related to the same shall be given in Section 5.

5. Intelligent heuristic optimization techniques

For the purpose of optimization of the above defined single objective functions, several numbers of optimization techniques are utilized, to have a comparative study. They include some of the more common conventional algorithms like LP [14] and intelligent heuristic search based algorithms like the GA [11] and the PSO [12], etc. A recently proposed intelligent technique based algorithm known as the CSA is also utilized for the purpose of optimization. All the optimization methods used in optimizing a single objective function formulated by combining different objectives, sometimes fail to give a robust solution, as they tend to oversimplify the process of formulation of an objective function. Therefore a multi objective optimization solution is obtained using the NSGA-II. From the results the relative merits of using a method of multi-objective optimization, may be compared to those obtained with the single objective function based optimization methods. A brief discussion related to two of the above optimization methods i.e., CSA and NSGA-II shall be presented here.

5.1. Cuckoo Search Algorithm (CSA)

The CSA is an evolutionary algorithm that is inspired by the *brood parasitism* found in the breeding behavior of some

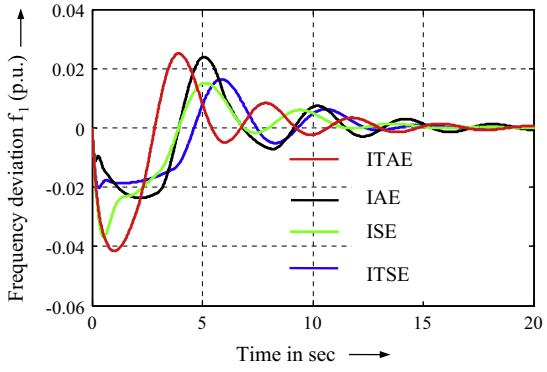

Figure 4 Frequency behaviors for 2% load change in 1st area for different objective functions.

commonly found species of cuckoos. The algorithm is structured by following the mathematical model of the behavior of L'evy flight found in some birds and fruit flies [13]. For using the algorithm in the present work, three simplifying assumptions described below are applied. They are as follows

(i) Each cuckoo lays one egg at a time which it dumps in a randomly selected nest.
(ii) The best nests having better quality eggs, are retained for subsequent generations
(iii) Keeping the total numbers of host nests as constant, an egg laid by a cuckoo could be detected by the host bird with a probability (P_a) of 0.1.

In the methodology, each egg in a nest represents a potential solution of optimizing variables along with its fitness value equal to the value of the concerned objective function. During the course of optimization, the aim is to find cuckoos with better solutions in place of already existing solutions in the nests.

5.2. Multi-objective optimization with NSGA-II

An optimization problem having multiple objectives can be formulated simplistically as a single objective problem as weighted sum of the individual objectives with suitably selected weights for each of them. However, a misjudgment in the ratio of different weights would skew the eventual solution more toward one among all the objectives. On the other hand, there is a better chance of obtaining a more promising solution after suitably identifying it from those available from the set of Pareto optimal solutions. The later can be obtained with the help of a multi-objective optimization algorithm like NSGA-II. The flowchart of NSGA-II is given in Fig. 5. The algorithm is a modified and improved version of NSGA and provides a set of compromise solution from all the non-inferior alternatives. Finally, the process of choosing the most suitable non dominant solution not only becomes problem dependent but also varies with the preference of the decision maker. Therefore, the final solution to the problem is the result of both an optimization process and a decision process. In the present paper, a fuzzy-based membership value assignment approach is applied to select the best compromise solution from the obtained Pareto set. In this method, the ith objective function of a solution in a Pareto set is assigned a membership value μ_i defined as follows [24].

$$\mu_i = \begin{cases} 1, & K_i \leqslant K_i^{\min} \\ \frac{K_i^{\max} - K_i}{K_i^{\max} - K_i^{\min}}, & K_i^{\min} < K_i < K_i^{\max} \\ 0, & K_i \geqslant K_i^{\max} \end{cases} \quad (4)$$

where $K_i^{\max}$ and $K_i^{\min}$ are the maximum and minimum values of the ith objective function, respectively. For each solution i, the membership value μ^j is calculated as:

$$\mu^j = \frac{\sum_{i=1}^{n} \mu_i^j}{\sum_{j=1}^{m} \sum_{i=1}^{n} \mu_i^j} \quad (5)$$

where n is the number of objectives functions and m is the number of solutions. The solution having a membership value close to the highest membership value μ^j is chosen as the best compromise solution [24].

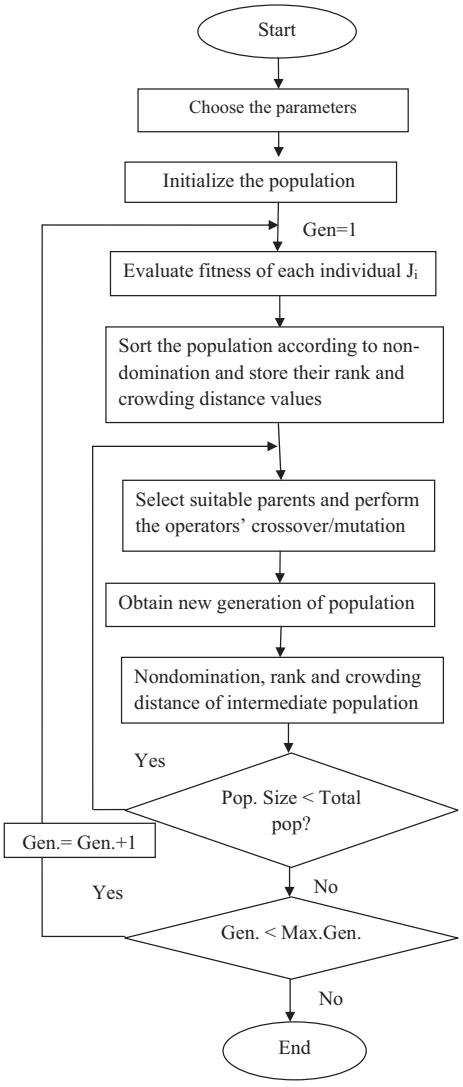

Figure 5 Flowchart of non-dominated sorting genetic algorithm-II.

6. Simulations and results

The simulations are performed in the two area system mentioned earlier using MATLAB/Simulink. Further, the study assumes that the size and capacities of the converters and the controllers utilized in the DFIG of the wind power system are identical in both the areas. The local factors and disturbances related to each area do not alter them in any condition. In many previous researches related to this work, the practice has been to give 20% of wind power support replacing equivalent amount of thermal powers [3,10] from the systems. The optimization of objective functions assumes the same condition, even though the tuned controllers are tested for their performance with changes in the level of wind penetration. The system data are obtained from the work in [25], and they are mentioned in Appendix A. It can be seen from the simulation model shown in Fig. 3 that, there are five numbers of controller parameters, K_i K_{pf}, K_{df}, K_{wp}, and K_{wi}. To reduce the computational burden, it is decided to optimize smaller numbers of controller gains among all. For choosing the more

sensitive gains among them, a sensitivity study is carried out as follows.

In the sensitivity analysis, at the outset, the system load is changed in a step of 2% in the 1st area. Keeping the values of other gains constant, for an incremental change of 1% in each of the controller gains, the corresponding change in the values of any of the widely utilized performance indices is evaluated separately. The sensitivity values of each of the gains toward different performance indices are given in Table 2.

From Table 2, it is clear that the gains K_i, K_{df} and K_{pf} are more sensitive compared to the remaining two gains, toward each of the performance index. Therefore, these three gains are decided to be optimized using different optimization algorithms.

6.1. NSGA-II tuned controller parameters (K_i, K_{df}, K_{pf})

It may be observed that, both the control areas have equal capacities and they are assumed to have identical model parameters. Therefore, the values of the controller parameters K_i, K_{df}, K_{pf} to be optimized, are assumed to be of identical values in both the areas. The T_s, $1/x$ and ITSE values of the system are three separate performance indices which are considered as three multiple objectives for optimization. A 2% step perturbation of real power loads (P_d) of the 1st control area, from its respective nominal value, is simulated to obtain the three objective functions. The optimized values of the controller parameters and their respective multiple objective functions are obtained after the convergence of the algorithm. In each generation the population size is kept at 40. At the end of every generation, ten members of the population out of all, whose membership values μ^j are the highest among all the members, are retained. The optimal controller parameters and the corresponding optimized values of the objective functions, obtained above are highlighted, in Table 3. Fig. 6 depicts the values of the three different objectives obtained for all the 10 best population after the convergence of the optimization process.

Table 2 Values of sensitivity of different controller gains toward different performance indices.

	Ki	Kwp	Kwi	Kpf	Kdf
ISE	0.0031	0.0003	0.0021	0.0019	0.0017
IAE	0.1737	0.0104	0.0654	0.0150	0.0019
ITSE	0.0146	0.0009	0.0083	0.0011	0.0020
ITAE	0.7259	0.0879	0.1052	0.4543	0.3993
Weighted sum of above performance indices	0.2653	0.0052	0.0359	0.0408	0.1617

Maximum sensitivity
2nd most sensitivity
3rd most sensitivity

6.2. Comparison of NSGA-II with other optimization technique

A comparison between NSGA-II and other widely accepted optimization techniques like CSA, LP, PSO and GA is also sought in this work. The objective function J is considered to be optimized with all the above optimization techniques which essentially optimize an objective function having one objective. It may be seen that, J is formulated by combining the same three numbers of individual objectives, which are also evaluated individually in the multi objective optimization with NSGA-II. The weighing factors ω_1, ω_2 and ω_3 are suitably chosen to give equal weight to each of the three objectives after addition to form J. The optimization algorithms used for this work are all well established, the parameters adopted with each of them, is given in Appendix A. Table 4 depicts the parameter values of the three optimized gains, obtained with the above discussed single objective based optimization techniques.

The time domain responses of frequencies Δf_1, Δf_2, of both the areas and the tie line power deviations ΔP_{Tie}, obtained for a SLP of 2% in the 1st area, using the optimized controllers for all the above optimization techniques, are shown in Fig. 7.

Further, to have a comparison all the performance indices including those not considered in the process of optimization i.e., ISE, IAE and ITAE are also obtained. These performance indices are obtained for each of the optimized controllers

Table 3 The values of optimized controller parameters and their objective function values, for the best ten solutions of Pareto Set obtained in the last generation NSGA-II.

NSGA-II: solutions/parameter	Controller parameters			Total settling time in s (T_s)	Minimum damping ratio (MDR)	ITSE
	K_i	K_{df}	K_{pf}			
1st (Best)	0.834583	0.217337	0.0825339	64.56	0.2554	0.0056542
2nd	0.852748	0.228261	0.0838724	65.72	0.2494	0.00542745
3rd	0.775711	0.173426	0.0893795	87.98	0.2880	0.00683781
4th	0.781328	0.185137	0.0812082	78.97	0.2747	0.00647375
5th	0.818847	0.208410	0.080668	68.32	0.2600	0.00585503
6th	0.837267	0.338364	0.0233076	98.49	0.1512	0.00449175
7th	0.783754	0.183634	0.0859591	81.52	0.2779	0.00653582
8th	0.792488	0.192974	0.0781764	72.71	0.2688	0.00623686
9th	0.805263	0.344084	0.0277726	90.03	0.1394	0.00469071
10th	0.818844	0.346273	0.025922	92.2	0.1413	0.004579

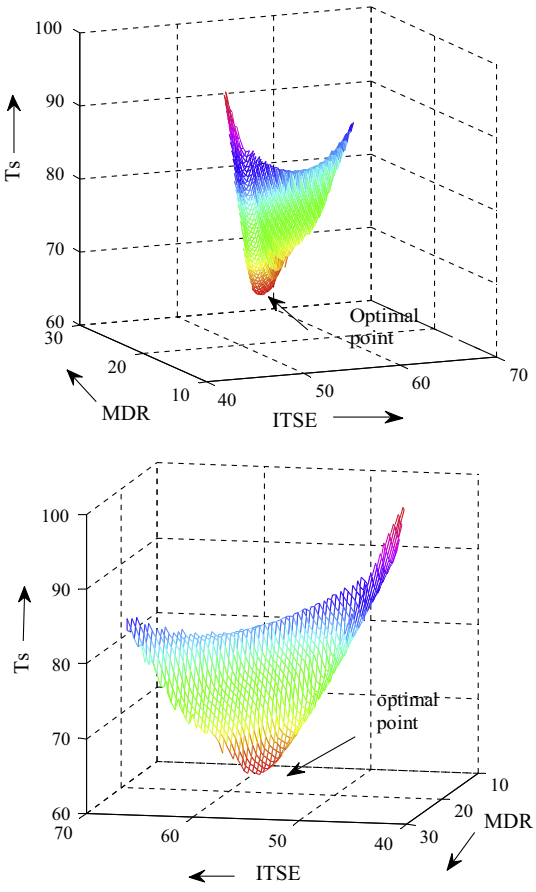

Figure 6 Sorted objective function values of best 10 solutions at the point of convergence.

separately with NSGA-II, CSA, LP, PSO and GA. Moreover as depicted in Table 5, the performance indices with the NSGA-II optimized controller, are better compared to those obtained with others. In the results obtained with other optimization algorithms, it is seen that, even though some of them have given better values of a particular performance indices compared to the NSGA-II, but deteriorated other ones. Therefore, the NSGA-II has provided better performing controllers compared to others. The values of 10 best solutions at the point of convergence are shown in Fig. 6.

6.3. Response of DFIG controller with different levels of wind penetration (L_p)

An event is simulated in which the two area system is subjected to the same SLP of 2% in the first area. Depending upon the

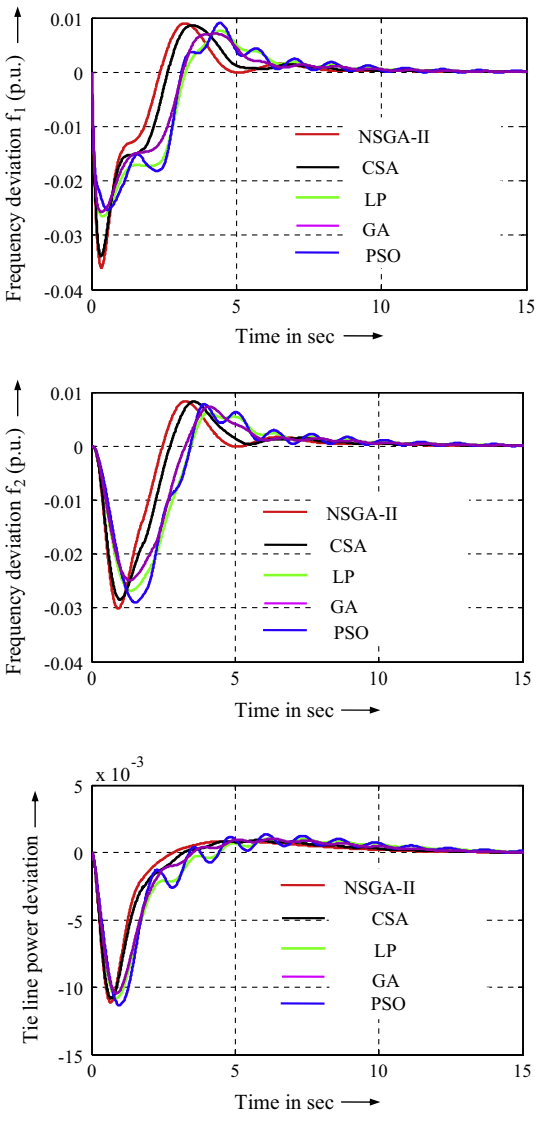

Figure 7 Grid frequency and tie line power deviations for a 2% load change in the 1st area obtained with different schemes of controllers.

operational scenario, availability of wind and any other extraneous factor, the frequency support capability of DFIG may be utilized in varied degrees. Therefore, the tuned controllers should be tested for their ability to show some robustness with variation in the penetration level (L_p). For different values of L_p, the changes in the values of H and R are given in Table 1. However, even with the variation of the above values,

Table 4 Controller parameters and their *PFIs* obtained with different single and multi objective methods.

Optimization method/parameter	Controller parameters			Total settling time in se c (T_s)	Minimum damping ratio (MDR)	ITSE
	K_i	K_{df}	K_{pf}			
NSGA-II:1	0.83458	0.217337	0.08253	64.56	0.2554	0.005654
CSA	0.7218	0.2512	0.0975	70.90	0.2963	0.0069
LP	0.5172	0.3106	0.1959	78.91	0.1766	0.0106
PSO	0.5412	0.2723	0.2902	84.31	0.1755	0.0109
GA	0.6092	0.3428	0.1973	73.66	0.2897	0.0085

Table 5 Comparison of several *PFIs* and MDR of the system with controllers tuned with.

Performance indices		Comparison of different optimization technique				
		NSGA-II	CSA	LP	PSO	GA
ISE		0.0032	0.0034	0.0040	0.0040	0.0034
IAE		0.2058	0.2285	0.2807	0.2750	0.2520
ITAE		0.7519	0.8994	1.3164	1.2773	1.1302
T_s (s)	Δf_1	22.3400	24.5300	27.0300	29.0800	25.3700
	Δf_2	23.3200	25.5600	28.1500	30.0900	26.4500
	ΔP_{tie}	18.9000	20.8100	23.7300	25.1400	21.8400
Eigen values		1.0e + 002×	1.0e + 002×	1.0e + 002×	1.0e + 002×	1.0e + 002×
		−0.0625 ± 0.0313i	−0.0603 ± 0.0379i	−0.0610 ± 0.0732i	−0.0626 ± 0.0947i	−0.0604 ± 0.0732i
		−0.0651 ± 0.0348i	−0.0637 ± 0.0411i	−0.0645 ± 0.0732i	−0.0653 ± 0.0939i	−0.0639 ± 0.0731i
		−0.0118 ± 0.0241i	−0.0134 ± 0.0216i	−0.0089 ± 0.0150i	−0.0051 ± 0.0140i	−0.0092 ± 0.0143i
		−0.0226 ± 0.0071i	−0.0243 ± 0.0071i	−0.0027 ± 0.0014i	−0.0026 ± 0.0014i	−0.0020 ± 0.0012i

the damping controllers tuned for levels of 20% penetration should not alter their response adversely to destabilize the system. The values of the controller parameters obtained from NSGA-II are kept constant for changes in L_p. The deviation of frequency obtained for different wind penetration levels from 0% to 50% is shown in Fig. 8. It can be noticed that with low wind penetration there is no significant variation but it is observed that with higher values of the L_p, the settling time will be longer.

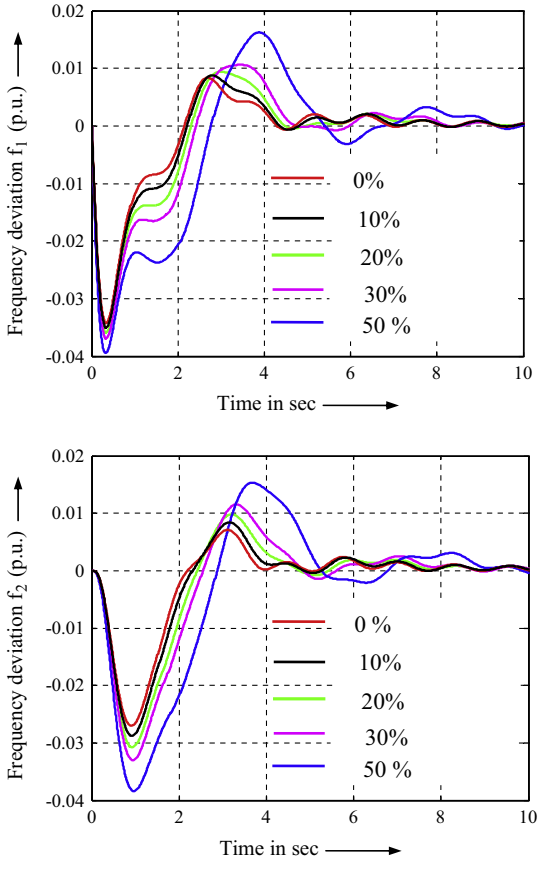

Figure 8 Area frequencies for different levels of L_p with NSGA-II controllers having frequency support.

6.4. Improvement frequency regulation with wind penetration

To further investigate into the relative performance of wind power over thermal power in terms of their abilities in providing frequency regulation in the test system, three separate scenarios of real power generation are compared. They are as follows

- First case 20% wind power with the ability of frequency support.
- In second case 20% wind power without frequency support.
- In third case, no wind penetration in the thermal system.

Under all the above circumstances, optimization of the controller parameters is carried out using NSGA-II. The optimized parameter values and three of the performances indices are given comparatively in Table 6.

For a 2% disturbance in the load in the 1st area, the behavior of the frequency and tie-line power deviations are obtained for the above three cases, which are shown in Fig. 8. It can be observed from Fig. 9, that the dynamic performance in terms of the frequency and tie line power deviations of both the areas are better with the first case compared to the other two cases. Moreover, the third case of providing wind power without having a frequency support capability has resulted in worst dynamic performance as the overall inertia of the system has reduced with wind power contribution. As expected, similar results are also obtained in terms of different performance indices as given in Table 6.

6.5. Controller performance evaluation for different disturbances and changes in parameters

6.5.1. Step load increase in different area

The optimized controller parameters of both the areas are set at their optimized values obtained with NSGA-II. Both the control areas are subjected to a 2% of SLP from the nominal value, first individually in each area and then simultaneously in both the areas. Dynamic response of Δf_1, Δf_2 and ΔP_{Tie} obtained for each of the perturbations is depicted in Fig. 10. It can be seen that, both the area frequency deviations become more when loads in both of them increase simultaneously. Moreover, as similar step load perturbations are given in two similar areas, the tie line power deviation remains zero.

Table 6 Performance evaluation for with/without DFIG and DFIG with f-support.

Type of power generation	Controller parameters			ITSE	T_s			MDR
	K_i	K_{df}	K_{pf}		Δf_1	Δf_2	ΔP_{tie}	
Thermal-wind with frequency support	0.834583	0.217337	0.0825339	0.0057	22.34	23.32	18.90	0.2554
Thermal	0.5122	0	0	0.0108	25	26	21.95	0.0784
Thermal-wind without frequency support	0.3440	0	0	0.0226	29.47	32.58	30.18	0.0649

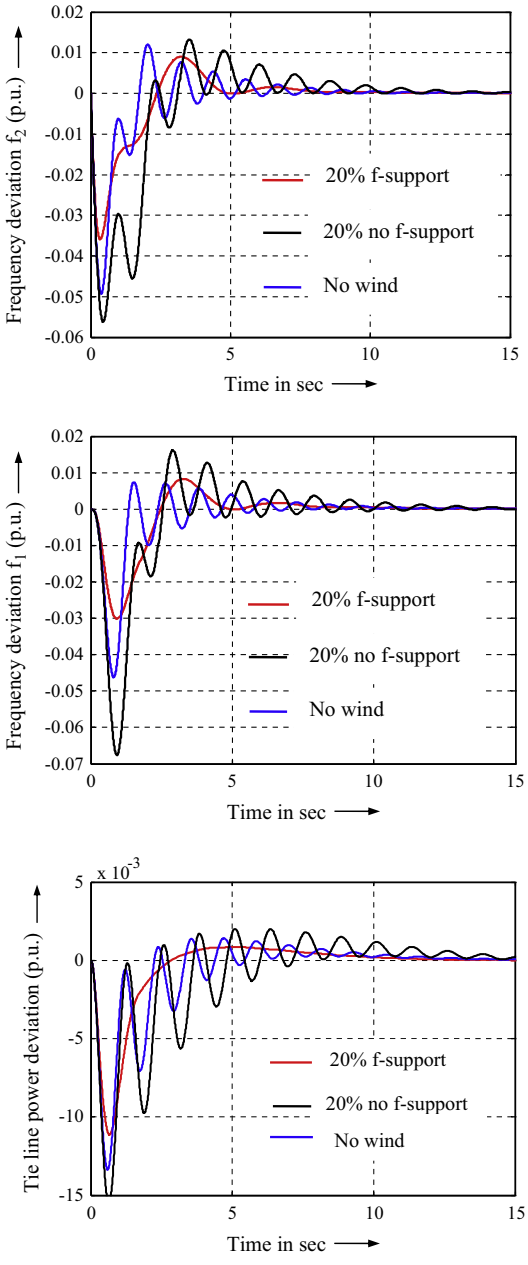

Figure 9 Δf_1, Δf_2 and ΔP_{Tie} for with and without frequency support capability of DFIG.

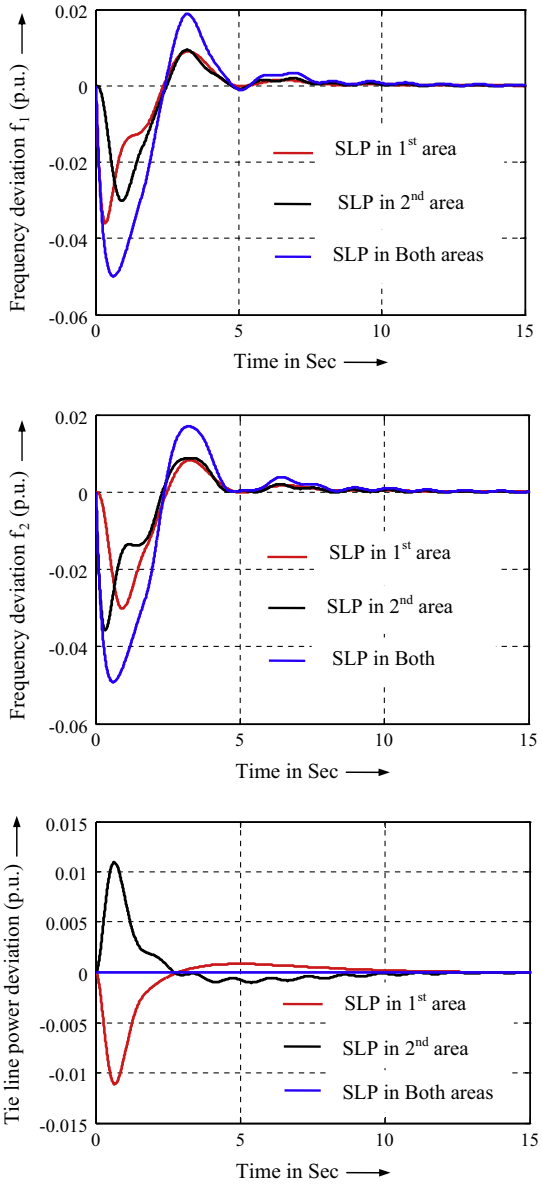

Figure 10 Δf_1, Δf_2 and ΔP_{Tie} for 2% SLP in different areas created as separate events.

6.5.2. Sensitivity analysis with variation in parameter& operating conditions

In order to examine the robustness of the tuned controllers for variations in the system parameters and the operating conditions, they are changed in wide ranges. First, to test the robustness of controllers toward parameter variations, several numbers of time constants related to the washout filter (T_w), frequency transducer (T_R), controlled WECS (T_A) are varied in the range of −50% to +50% from their respective nominal values. The values of ITSE, T_s of Δf_1, Δf_2 and ΔP_{Tie} for both the areas and the MDR obtained with variations in the system parameters are listed in Table 7. The controller performances

Table 7 Sensitivity analysis.

Parameter variation	% Change	Performance index ITSE	Settling time			MDR
			Δf_1	Δf_2	ΔP_{tie}	
	Nominal	0.0057	22.34	23.32	18.90	0.2554
Washout filter time const (T_w)	+50	0.0054	27.43	28.40	19.62	0.2429
	+25	0.0055	25.35	26.36	19.59	0.2463
	−25	0.0059	28.32	29.32	20.39	0.2819
	−50	0.0065	39.03	38.06	26.57	0.4187
Frequency transducer time const (T_R)	+50	0.0055	29.35	28.38	21.34	0.2541
	+25	0.0056	25.10	26.09	19.39	0.2547
	−25	0.0057	26.12	27.12	20.24	0.2561
	−50	0.0059	30.36	31.31	22.22	0.2569
WECS time const (T_A)	+50	0.0055	33.78	34.77	23.52	0.2391
	+25	0.0056	29.39	30.33	21.37	0.2471
	−25	0.0059	30.40	31.37	22.27	0.2641
	−50	0.0062	37.02	37.99	26.52	0.2732
Equivalent WECS inertia (H_e)	+50	0.0055	27.47	26.53	19.70	0.2591
	+25	0.0056	25.33	26.32	19.59	0.2603
	−25	0.0058	28.33	29.30	20.42	0.2499
	−50	0.0062	36.96	35.95	24.60	0.2586

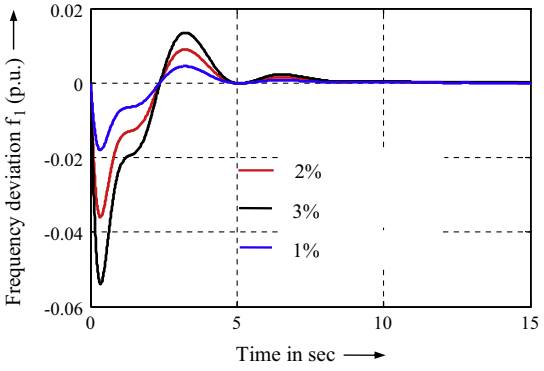

Figure 11 Δf_1 for additional ±1% SLP in the 1st area.

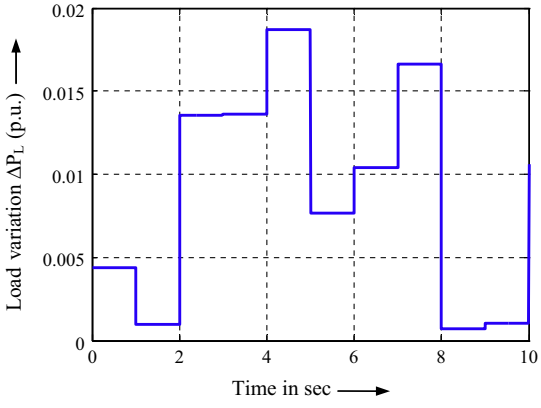

Figure 12 Pattern of random values of SLP.

have remained stable even with variation in the above time constant parameters. Further, the variations in the values of equivalent WECS inertia constant (H_e), have not degraded the performances of the optimized controllers.

To test the robustness with the change in operating condition, another 1% perturbation in the load demand of 1st area in addition to the existing 2%, is introduced. The additional perturbation of 1% is simulated both by increasing and decreasing from the existing value of 2%. The frequency deviations obtained at these new operating points are depicted in Fig. 11. It can be seen that even with the variation of operating condition at which the controllers were tuned, the dynamic performance of the NSGA-II tuned controller has not altered significantly.

The tuned controllers are further tested, when the defined SLP of 2% is made to change randomly in different degrees in range of a 0–2% with time. The above variation of load for different intervals of time is shown in Fig. 12. The frequency deviations obtained at these new operating points are depicted in Fig. 13.

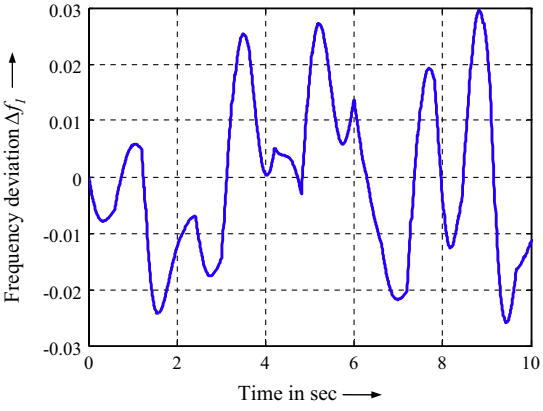

Figure 13 Δf_1 for the random SLP in the 1st area.

6.6. Discussions

It may be inferred that, when the DFIG based wind power does not provide frequency support, the frequency deviation is more due to the case of decrease of overall inertia of the system. But the modified inertia control of the DFIG allows kinetic energy stored by rotational mass to improve frequency support. The response of the conventional generators is considerably slower than that of the wind turbine equivalent generation when the frequency support capability is available from the later.

7. Conclusion

The work aims to optimize the controller gains of DFIG and AGC simultaneously in a coordinated manner. The fast response capability associated with electronically controlled PD control loop of DFIG based WECS is utilized to improve the transient performance of frequency regulation of power system. Integrated with thermal systems, a coordinated tuning of the PD controllers along with those of integral controllers of AGC in a two area is found to be beneficial. The tuning of controller parameters is carried out using a multi-objective optimization to find the set of controllers whose performance show non domination and improve many performance indices without deteriorating others. The controllers with NSGA-II are also found to be better compared to similar controllers optimized with some recently published modern heuristic optimization techniques i.e., Cuckoo Search Algorithm (CSA), Linear Programming, Genetic Algorithm (GA) and Particle Swarm Optimization (PSO), in terms of their robustness. The new controllers depict better ability of disturbance rejection, when system parameters and operating conditions are varied. One of the motivations of optimizing the gains of wind and thermal systems using a multi-objective optimization NSGA-II, was to examine the efficacy of the same for tuning the gains of two systems having different characteristics of inertial response. The overall dynamic performance of the controllers optimized with NSGA-II has shown better results compared to those obtained with the single objective based optimization methods.

Appendix A

A.1. Nominal parameter of system investigated [25]

i = Subscript referred to area (1,2)
H_i = Inertia constant of area i, $H_1 = H_2 = 5$
Δf_i = Incremental change in frequency of area i (Hz)
ΔP_{d_i} = Incremental load change in area i (p.u.)
$D_i = \Delta P_{d_i}/\Delta f_i = 8.33 \times 10^{-3}$ p.u. MW/HZ
ΔP_{g_i} = Incremental generation change in area i (p.u.)
$\Delta P_{tie_{i-j}}$ = Incremental change in tie-line power of tie-line i–j (p.u.)
R_i = Governor speed regulation parameter of area i, $R_1 = R_2 = 2.4$ (HZ/p.u. MW)
T_{g_i} = Steam governor time constant of area i, $T_{g1} = T_{g2} = 0.08$ s
K_{r_i} = Steam turbine reheat coefficient of area i, $K_{r1} = K_{r2} = 0.5$
T_{r_i} = Steam turbine reheat time constant of area i, $T_{r1} = T_{r2} = 10$ s
T_{t_i} = Steam turbine time constant of area i, $T_{t1} = T_{t2} = 0.3$ s
β_i = Frequency bias of area i $(D_i + \frac{1}{R_i})$, $\beta_1 = \beta_2 = 0.425$
f_i = Nominal system frequency of area i (Hz), $f_1 = f_2 = 60$ HZ.
T_{p_i} = Power system time constant of area i
$T_{p1} = T_{p2} = 20$ s$(T_p = \frac{2H}{fD})$
$K_{p_i} = \frac{1}{D_i}$ = Power system gain constant of area i, $K_{p1} = K_{p2} = 120$ HZ/p.u. MW,$(K_p = \frac{1}{D})$
T_{ij} = Synchronizing coefficients, $T_{12} = 0.0867$ s

Total rated area capacity, $P_{r1} = P_{r2} = 2000$ MW

$a_{12} = -\frac{P_{r1}}{P_{r2}}$ = (P_{ri} = rated area capacity)
ITAE = Integral of time multiple of absolute error
$\text{ITAE} = \int_0^{t_{\text{sim}}} t[|(\Delta f_1)| + |(\Delta f_2)| + |(\Delta P_{Tie})|] \cdot dt$
$\text{IAE} = \int_0^{t_{\text{sim}}} [|(\Delta f_1)| + |(\Delta f_2)| + |(\Delta P_{Tie})|] \cdot dt$
ITSE = Integral time square error,
$\text{ITSE} = \int_0^{t_{\text{sim}}} t[(\Delta f_1)^2 + (\Delta f_2)^2 + (\Delta P_{Tie})^2] \cdot dt$
$\text{ISE} = \int_0^{t_{\text{sim}}} [(\Delta f_1)^2 + (\Delta f_2)^2 + (\Delta P_{Tie})^2] \cdot dt$

A.2. Nominal parameter of system with DFIG [9]

R and H changes, so for 20% penetration of DFIG

β_i = Frequency bias of area i $(D_i + \frac{1}{R_i})$, $\beta_1 = \beta_2 = 0.3417$
T_{p_i} = Power system time constant of area i, $T_{p1} = T_{p2} = 18.8415$ s$(T_p = \frac{2H}{fD})$.
H_e = Equivalent WECS inertia = 3.5 s
T_w = Washout filter time constant = 6 s
T_R = Frequency transducer time constant = 0.1 s
T_A = Controlled WECS time constant = 0.2 s
K_{pw} = Speed regulator proportional constant = 1.5
K_{iw} = Speed regulator integral constant = 0.15
$P_{NC}^{\min}/P_{NC}^{\max}$ = WECS output power limit = 0/1.2 p.u.

A.3. PSO parameters

Number of particles = 20 $C_1 = 1.2$, $C_2 = 1.2$, Moment of inertia = 0.9
Maximum number of step = 20, Dimension of the problem = 3

A.4. CSA parameters

n = numbers of nests = 15
P_a = probability of detection an egg by the host bird = 0.1
n_d = number of optimizing variable = 3

A.5. GA parameters

Initial Population Size – 50, Elitism – 2
Selection – Roulette wheel; Crossover Probability – 0.92
Cross Over Function – multiple point
Mutation Probability – 0.05

References

[1] Wind turbines connected to grids with voltages above 100 kV – technical regulation for the properties and the regulation of wind turbines. Elkraft System and Eltra Regulation, Draft version TF 3.2.5; December 2004.

[2] European Wind Energy Association (EWEA). Large scale integration of wind energy in the European power supply: analysis, issues and recommendations; 2005. Available: <http://www.ewea.org/>.

[3] Ullah NR, Thiringer T, Karlsson D. Temporary primary frequency control support by variable speed wind turbines – potential and applications. IEEE Trans Power Syst 2008;23(2):601–12.

[4] Mullane A, O'Malley M. The inertial response of induction machine based wind turbines. IEEE Trans Power Syst 2005;20(3):1496–503.

[5] Lalor G, Mullane A, O'Malley M. Frequency control and wind turbine technologies. IEEE Trans Power Syst 2005;20(4):1905–13.

[6] Anaya-Lara O, Hughes FM, Jenkins N, Strbac G. Contribution of DFIG-based wind farms to power system short-term frequency regulation. Proc Inst Elect Eng Gen Transm Distrib 2006;153(2):164–70.

[7] Morren J, de Haan SWH, Kling WL, Ferreira JA. Wind turbines emulating inertia and supporting primary frequency control. IEEE Trans Power Syst 2006;21(1):433–4.

[8] Almeida RG, Lopes RG. Participation of doubly fed induction wind generators in system frequency regulation. IEEE Trans Power Syst 2007;22(3):944–50.

[9] Mauricio JM, Marano A, Gómez-Expósito A, Martínez RJL. Frequency regulation contribution through variable-speed wind energy conversion systems. IEEE Trans Power Syst 2009;24(1):173–80.

[10] Bhatt P, Roy R, Ghoshal SP. Dynamic participation of doubly fed induction generator in automatic generation control. Sci Direct Renew Energy 2011;36:1203–13.

[11] Aditya SK, Das D. Design of load frequency controllers using genetic algorithm for two area interconnected hydro power system. Elect Power Comp Syst 2003;31(1):81–94.

[12] Ghoshal SP. Optimizations of PID gains by particle swarm optimizations in fuzzy based automatic generation control. Electric Power Syst Res 2004;72:203–12.

[13] Yang XS, Deb S. Cuckoo search via Ĺevy flights. Proc. of World Congress on Nature & Biologically Inspired Computing (NaBIC 2009) 2009, India. IEEE Publications, USA.

[14] Zhang Yin. Solving large-scale linear programs by interior-point methods under the Matlab* Environment. Opt Methods Softw 1998;10(1):1–31.

[15] Deb K, Pratap A, Agarwal S, Meyarivan T. A fast elitist multi-objective genetic algorithm: NSGA-II. IEEE Trans Evol Comput 2002;6:182–97.

[16] Naidu K, Mokhlis H, Bakar AHA. Multi-objective optimization using weighted sum artificial bee colony algorithm for load frequency control. Electr Power Energy Syst 2014;55:657–67.

[17] Yingcheng X, Nengling T. Review of contribution to frequency control through variable speed wind Turbine. Elsevier Renew Energy 2011;36:1671–7.

[18] Chan ML, Dunlop RD, Schweppe F. Dynamic equivalents for average system frequency behaviour following major disturbances. IEEE Trans Power Appl Syst Jul. 1972;91(4):1637–42.

[19] Almeida RG de, Castronuovo E, Lopes J. Optimum generation control in wind parks when carrying out system operator requests. IEEE Trans Power Syst 2006;21(2):718–25.

[20] Hughes FM, Anaya-Lara O, Jenkins N, Strbac G. Control of DFIG-based wind generation for power network support. IEEE Trans Power Syst 2005;20(4):1958–66.

[21] Goldberg DE. Genetic algorithms in search, optimization, and machine learning. Boston: Addison-Wesley; 1989.

[22] Srinivas N, Deb K. Multi-objective optimization using non-dominated sorting in genetic algorithms. IEEE Trans Evol Comput 1994;2:221–48.

[23] Panda S, Yegireddy NK. Automatic generation control of multi-area power system using multi-objective non-dominated sorting genetic algorithm-II. Int J Electr Power Energy Syst 2013;53:54–63.

[24] Abido MA, Bakhashwain JM. Optimal VAR dispatch using a multiobjective evolutionary algorithm. Int J Electr Power Energy Syst 2005;27:13–20.

[25] Elgerd 0I. Electric energy systems theory: an introduction. McGraw-Hill, 2nd ed.; 2005 [25th Reprint].

Mrs. S. Chaine received the B.E. From Government College of Engineering, Keonjhar, India in 2005 and M.Tech degree from the Biju Pattnaik University of Technology, Rourkela, Odisha, India in 2011. She is currently pursuing the Ph.D. degree in the Department of Electrical Engineering, Veer Surendra Sai University of Technology, Burla, Odisha, India. Her current research interests include power system operation and control.

Dr. M. Tripathy received the B.E. degree from N.I.T. (Formerly Regional Engineering College), Rourkela, India, in 1991, and worked in Industry for five years before completing M.E. from V.S.S.U.T (Formerly University College of Engineering), Burla in the year 2001. He completed Ph.D. from Indian Institute of Technology, Delhi, India in the year 2009. He has been a faculty in the Department of Electrical Engineering at. V.S.S.U.T, Burla in different capacities, as Lecturer during 2006–2010 and as a Reader since 2010. His field of interest is application of intelligent techniques to power system operation and control and wind energy conversion systems.

Mr. S. Satapathy received the B.Tech degree from Biju Pattnaik University of Technology, Rourkela, Odisha, India in 2011 and recently completed the M.Tech degree from Veer Surendra Sai University of Technology (VSSUT), Burla, India in 2014.